

# Production of 3D Tumor Models of Head and Neck Squamous Cell Carcinomas for Nanotheranostics Assessment

Melissa Santi,\* Ana Katrina Mapanao, Valentina Cappello, and Valerio Voliani\*



Cite This: *ACS Biomater. Sci. Eng.* 2020, 6, 4862–4869



Read Online

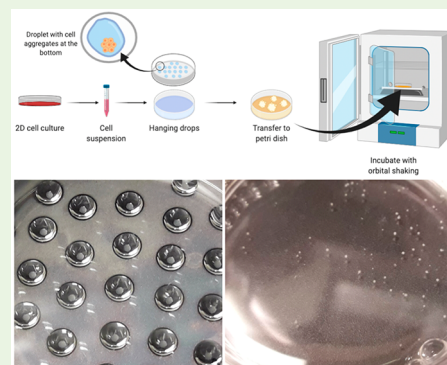
ACCESS |

Metrics & More

Article Recommendations

**ABSTRACT:** As a first approach, standard 2D cell culture techniques are usually employed for the screening of drugs and nanomaterials. Despite the easy handling, findings achieved on 2D cultures are often not efficiently translatable to *in vivo* preclinical investigations. Furthermore, although animal models are pivotal in preclinical studies, more strict directives have been implemented to promote the use of alternative biological systems. In this context, the development and integration into preclinical research workflow of 3D neoplasm models is particularly appealing to promote the advancement and success of therapeutics in clinical trials while reducing the number of *in vivo* models. Indeed, 3D tumor models bridge several discrepancies between 2D cell culture and *in vivo* models, among which are morphology, polarity, drug penetration, osmolality, and gene expressions. Here, we comprehensively describe a robust and high-throughput hanging drop protocol for the production of 3D models of both Human Papillomavirus (HPV)-positive and HPV-negative head and neck squamous cell carcinomas (HNSCCs). We also report the standard cascade assays for their characterization and demonstrate their significance in investigations on these aggressive neoplasms. The employment of relevant 3D cancer models is pivotal to produce more reliable and robust findings in terms of biosafety, theranostic efficacy, and biokinetics as well as to promote further knowledge on HNSCC pathophysiology.

**KEYWORDS:** spheroids, head and neck carcinomas, hanging drop method, oncology, 3D models



## INTRODUCTION

Head and neck squamous cell carcinomas (HNSCCs) represent a wide class of aggressive neoplasms with high incidence.<sup>1</sup> They usually involve the area comprising the oral cavity to the pharynx. HNSCCs are mainly divided in two classes, depending on the presence or absence of Human Papillomavirus (HPV) infection in cells.<sup>2</sup> Indeed, the sensitivity to treatments is strictly dependent on the presence of the virus in which HPV-positive patients are typically more sensitive to standard therapies with respect to the HPV-negative ones.<sup>3</sup> Despite the associated severe systemic toxicities and suboptimal efficacy, the principal noninvasive treatments for HNSCCs are still radiotherapy and cisplatin-based chemotherapy.<sup>4</sup> In this context, some synergistic nanotherapeutics are especially significant to advance the standard of care.<sup>5</sup> In general, two-dimensional cell cultures (monolayer of cells) are the most employed systems for first-stage investigations on the safety and efficacy of therapeutics.<sup>6,7</sup> The usual protocols consist of cell seeding in appropriate plastic or glass supports together with a medium that promotes cell growth and maintenance. Two-dimensional (2D) cell cultures offer several advantages. For example, they are cheap, well-established, and user-friendly.<sup>8</sup> However, monolayer cultures do not fully mimic *in vivo* conditions, and they are biased by the culture settings (such as artificial cell-surface interactions),

limiting the reliability of novel treatment evaluation as well as pharmacokinetics investigations.<sup>9</sup> Thus, accessible models that can better represent tumors are instrumental for the progress of preclinical oncological investigations.<sup>10,11</sup> In this regard, three-dimensional (3D) cancer models are of particular interest to bridge the gap between *in vitro* and *in vivo* assessments.<sup>12</sup> Indeed, they are more complex than cell monolayers, closer resemble the neoplasms' behaviors, among which are the cell-to-cell and cell-to-matrix interactions as well as the different pathophysiological gradients.<sup>13,14</sup> Moreover, the development of customized 3D neoplasm models is in agreement with the 3R's concept and the rationalization of animal employment in research.<sup>15</sup> Among the 3D cancer models, multicellular tumor spheroids are especially appealing due to the availability of various preparation methods (Figure 1),<sup>7</sup> making these models readily accessible (Figure 1).<sup>16</sup> These techniques usually exploit the presence of scaffolds that induce individual cells to form a

Received: May 4, 2020

Accepted: July 1, 2020

Published: July 1, 2020



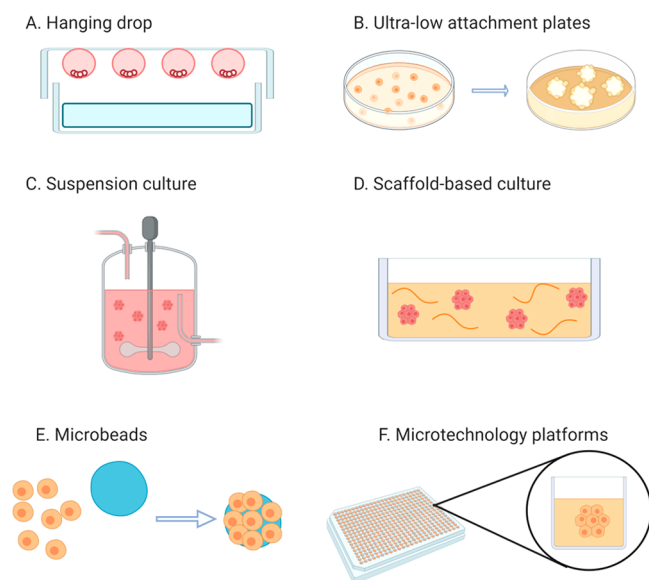


**Figure 1.** General scheme of the common techniques for spheroids production.

three-dimensional aggregate (e.g., scaffold-based culture and microbeads). However, scaffold-free methods (e.g., suspension culture, ultralow attachment plates, hanging drop, and microtechnology platforms) are preferred when high numbers of spheroids are needed. Among the production protocols, the hanging drop method can easily be applied to a wide range of cell lines, and the efficiency of spheroid formation relies on the inherent ability of the cells to self-aggregate.<sup>17</sup> In particular, it shows several advantages: (i) a simple setup, (ii) wide range of applications, and (iii) high reproducibility of spheroids with a narrow size distribution.

In this work, we report a standard protocol for the production of reliable spheroids of two HNSCCs cell lines, SCC-25 and UPCI:SCC-154, using a modified hanging drop method coupled with an orbital shaking procedure. This technique involves the formation of cell aggregates starting from a cell suspension that is dispensed as drops on the lid of a Petri dish, followed by the formation of the tridimensional structure from aggregates in an incubator with an orbital shaker. The protocol allows a massive production of reproducible multicellular tumor spheroids of these two particular cell lines.<sup>18</sup> SCC-25 and UPCI:SCC-154 are, respectively, HPV-negative and HPV-

positive squamous cell carcinomas. The 3D cultures of these cell lines represent good models to study oral malignancies, including the identification and evaluation of new therapies for the management of HNSCCs.<sup>19,20</sup> Moreover, some standard characterization assays, for the evaluation of the quality of the spheroids, among which optical microscopy techniques and transmission electron microscopy (TEM), are reported and comprehensively described.

## MATERIALS

### Reagents.

- Cell membrane marker (CellMask Green Plasma Membrane Stain, Thermo Fischer Scientific, C37608)
- Dulbecco's modified Eagle's medium (DMEM, Gibco, 31053028)
- DMEM/Ham's F12 1:1 medium (DMEM/F12 Gibco, 21041025)
- Fetal bovine serum, qualified, heat inactivated (FBS, Thermo Fisher Scientific, 10500064)
- Epoxy resin (Epon 812, Electron Microscopy Science, Hatfield, PA, USA)
- L-Glutamine (Thermo Fisher Scientific, A2916801)
- Glutaraldehyde 25% water solution (Electron Microscopy Science, Hatfield, PA, USA)
- HNSCC cell lines, SCC-25 and UPCI:SCC-154 (American Type Culture Collection, ATCC)
- Hydrocortisone (Sigma-Aldrich, H0888)
- Hoechst 33342 (Thermo Fisher Scientific, H3570)
- Sodium cacodylate trihydrate buffer (Sigma-Aldrich, C4945)
- Standard nanoarchitectures (NAs) conjugated with Alexa Fluor-647 fluorophore
- OsO<sub>4</sub> 4% water solution (Electron Microscopy Science, Hatfield, PA, USA)
- Potassium ferricyanide(III), K<sub>3</sub>Fe(CN)<sub>6</sub> (Sigma-Aldrich, 702587)
- Homemade staining solution (patent no. WO2019021201A1)
- Penicillin–streptomycin (Pen/Strep 100×, 5000 U/mL) (Thermo Fisher Scientific, 15070063)
- Phosphate-buffered saline without calcium and magnesium (PBS, Sigma-Aldrich, D8537)
- Trypsin-EDTA (0.5%), phenol red (Thermo Fisher Scientific, 25300054)
- Water, double distilled and autoclaved.
- General: pipet tips, centrifuge tubes, conical tubes, cell culture plates or flasks, serological pipettes, chambered coverglass for confocal imaging (e.g., Lab-Tek 8-well chamber, Thermo Fisher 155411).

### Equipment.

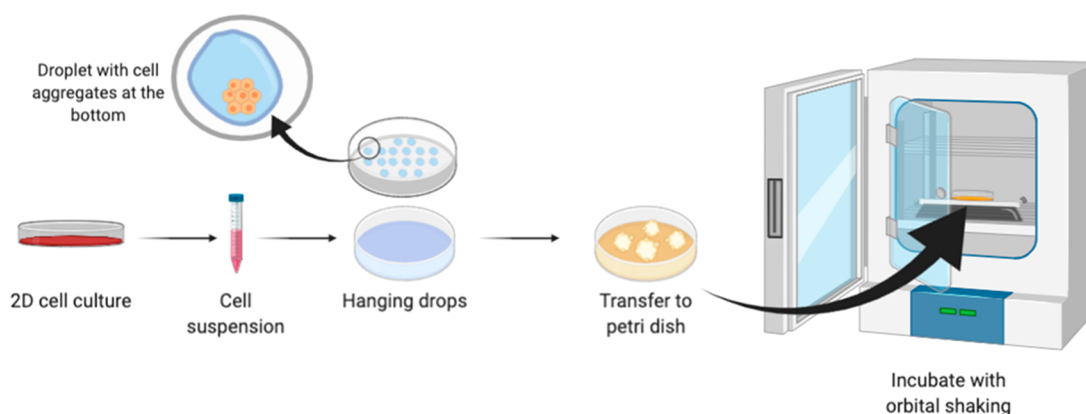


**Figure 2.** General scheme for spheroids production with the hanging drop method.

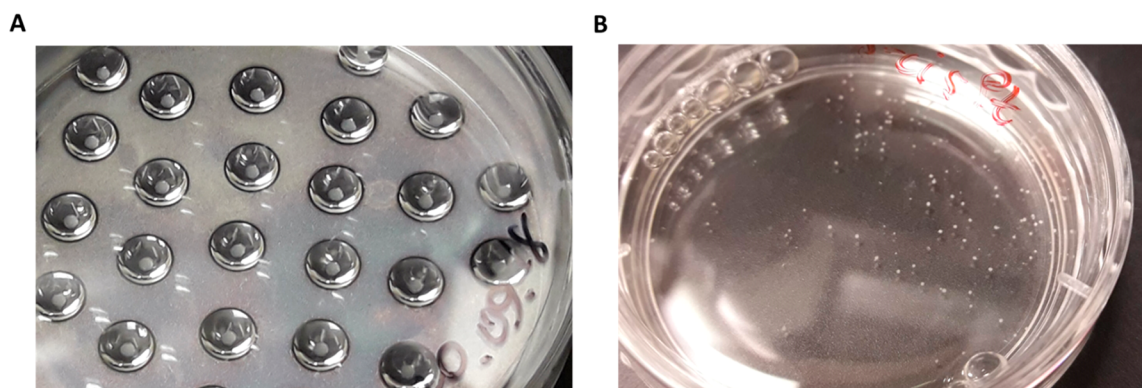


**Figure 3.** (A) Example of SCC-25 aggregates formed after 3 days of incubation in drops. (B) Spheroids of UPCI:SCC-154 cells after 24 h of shaking in the orbital incubator.

- Cell counter (Invitrogen Countess cell counter)
- Optical microscope
- Confocal microscope (Olympus FV1000)
- Ultramicrotome (UC7-Leica Microsystems, Vienna, Austria)
- Heater (working at 60 °C)
- Diamond knife 35° (DiATOME, Hatfield, PA, USA)
- Transmission Electron Microscope (TEM, ZEISS Libra 120 PLUS)
- Standard and orbital incubators (IncuSafe CO<sub>2</sub> incubators, Panasonic, 37 °C and 5% CO<sub>2</sub>)
- General: pipettors, incubators, BSL2-rated biosafety cabinet, centrifuges

## METHOD

### Overview.

- Step 1. Preparation of cell suspensions.
- Step 2. Preparation of drops to form cell aggregates.
- Step 3. Drops transfer and spheroids formation.
- Step 4. Spheroids recovery and preparation for employment.
- Step 5. Characterization of spheroids and data analysis.

**1. Preparation of Cell Suspensions.** The general scheme of the entire process is shown in Figure 2. Monolayer cell cultures have been established using previously described standard methods briefly reported below.<sup>21,22</sup>

- 1.1 For subculturing, SCC-25 cells were maintained in DMEM/F12 1:1 medium containing 1.2 g/L sodium bicarbonate, 2.5 mM L-glutamine, 15 mM HEPES, and 0.5 mM sodium pyruvate and supplemented with 400 ng/mL hydrocortisone. UPCI:SCC-154 cells were maintained in DMEM (high glucose: 4.5 g/L) containing 4 mM of L-glutamine. Both media were supplemented with Pen/Strep (final concentration 1×) and 10% FBS. Cells were plated in 100 mm tissue culture-treated dish, maintained in the static incubator at 37 °C and 5% of CO<sub>2</sub>, and split when 80–90% confluence was reached (every 3–4 days).
- 1.2 Cell suspensions of each cell line were prepared as described in the following. Medium was removed from the plate, and cells were washed with 5–10 mL of PBS to remove any serum residues. Then, cells were incubated with 2–3 mL of Trypsin-EDTA for 5–15 min and completely detached from the plate. Cells were diluted with 5 mL of medium, collected in a 15 mL conical tube, and centrifuged for 5 min at 1200 rpm. Then the medium was carefully removed, and cell pellet was resuspended with 3–5 mL of fresh medium. Note: The volume of medium may vary depending on the number of the cells. As an approximation, the bigger the pellet, the higher the amount of medium needed to resuspend the cells. Do not use more than 5 mL of medium to be sure to have the right concentration of cells for the next step.
- 1.3 Cells were counted using a cell counter system, and the concentration was adjusted to 1 × 10<sup>6</sup> cells/mL.

**2. Preparation of Drops to Form Cell Aggregates.** The formation of cell aggregates is the fundamental step to obtain optimal spheroids for subsequent experiments. The geometry and the final size of the spheroids strongly depend on the production and volume of the drops, as well as incubation time to allow the establishment of compact aggregates (Figure 3A).

The following procedure has been standardized for the preparation of SCC-25 and UPCI:SCC-154 spheroids with a diameter ranging from 200 to 400 μm by adapting other protocols.<sup>18</sup>

- 2.1 Standard plastic plates, without treatments for cell culture, can be used to produced drops. Here, we used 100 mm plate, and 10 mL of PBS was added to maintain the right humidity and avoid the dehydration of the drops.
- 2.2 The lid of the plate was flipped, and each cell suspension containing 1 × 10<sup>6</sup> cells/mL was well mixed with a pipet. Note that the cell suspension density is important for the success of the protocol. Then, we placed drops on the lid of the plate (Figure 3A). We used 10 and 20 μL of cell suspension for each drop of SCC-25 and UPCI:SCC-154, respectively. Note: the drops should be far enough apart to prevent any contact.
- 2.3 When the surface of the lid is completely covered by drops (Figure 3A), we flipped it carefully and put it on the plate and then in a static incubator at 37 °C and 5% of CO<sub>2</sub> until compact sheets were formed. For SCC-25 and UPCI:SCC-154, the process is 3 days long.

**3. Drop Transfer and Spheroid Formation.** After 3 days of static incubation, the compact aggregates are formed inside drops. Thus, they have to be transferred to a shaker in order to form the final tridimensional structure (Figure 3B).

- 3.1. Prepare a new 100 mm plates not treated for cell culture to prevent the attachment of sheets to the bottom of the plate once transferred.
- 3.2. Add 10 mL of fresh medium to the plate.
- 3.3. Carefully wash the lid containing drops with medium and move down the sheets inside the new plate with fresh medium. Note: sometimes during washing, the aggregates remain attached to the lid and do not fall into the new plate. They can be recovered by resuspending them using a pipet with some medium. This step must be done carefully to avoid aggregates disruption.
- 3.4. Place aggregates in an incubator with an orbital shaking stage for 24 h at 37 °C and 5% of CO<sub>2</sub>. Maintain the rotational speed between 60 and 80 rpm. Note: In general, the optimal speed for SCC-25 and UPCI:SCC-154 is 70 rpm.

**4. Spheroid Recovery and Preparation for Employment.** After 24 h incubation, spheroids should be ready to be recovered and characterized or employed for specific experiments. Here, we report how to manage spheroids for standard characterization and for the evaluation of nanomaterials.

- 4.1. Recover spheroids from the incubator with orbital shaker. If they are well-formed it is possible to observe them with the naked eye

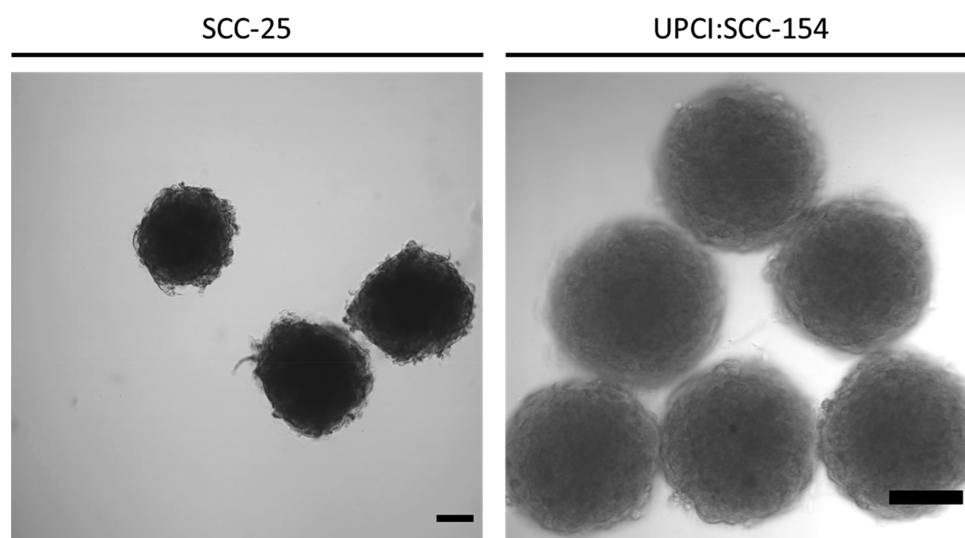


**Figure 4.** Optical images of SCC-25 and UPCI:SCC-154 spheroids after 24 h orbital shaking. Scale bar: 100  $\mu\text{m}$ .

(Figure 3B). Note: Spheroids can also be checked using an optical microscope (Figure 4).

- 4.2. Spheroids of SCC-25 and UPCI:SCC-154 are stable and can be easily taken using a pipet with a 1 mL tip. Note: Spheroids bigger than 600  $\mu\text{m}$  can get stuck at the top of the tip. In this case, you can cut the tip with sterilized scissors and easily recover spheroids without damaging them.
- 4.3. Transfer spheroids (the number of spheroids per tube is dependent on the experiment that you have to perform; in these cases, 3–5 spheroids are enough) to a 1.5 mL tube and treat them by following your specific experimental protocol. Here, we reported two types of experiments: (i) a TEM characterization and (ii) a confocal microscopy imaging for qualitative nanoparticle internalization evaluation. In the first one, samples from both cell lines were fixed using glutaraldehyde solution dissolved in sodium cacodylate buffer (0.1 M pH 7.4) at a final concentration of 1.5% v/v for 1 h at room temperature and then treated for a conventional embedding protocol.<sup>23</sup> Recovered spheroids were kept in a new fixative solution overnight at 4 °C. Then, the samples were postfixed for 1 h (1% OsO<sub>4</sub> plus 1% K<sub>3</sub>Fe(CN)<sub>6</sub> in sodium cacodylate buffer; 0.1 M pH 7.4) and stained with our homemade staining solution.<sup>24</sup> Finally, the spheroids were dehydrated in ethanol gradient and embedded in epoxy resin. Polymerization of the resin was carried out for 48 h at 60 °C. Then, 90 nm sections were obtained with UC7 ultramicrotome (Leica Microsystems, Vienna, Austria) equipped with a 35° diamond knife (DiATOME Hatfield, PA, USA) and collected on 300 mesh copper grids (Electron Microscopy Science, Hatfield, PA, USA). Sections were finally analyzed by TEM. Note: Spheroids usually maintain their structure and can be easily manipulated. For example, after the treatments, they can be washed several times with PBS without losing their features. In the second experiment, we treated the spheroids with gold nanoarchitectures produced as described elsewhere.<sup>25,26</sup> Spheroids were incubated with nanoparticles for 2 h at 37 °C and 5% of CO<sub>2</sub> in a static incubator. Then, nuclei (Hoechst 33342) and cell membrane markers (CellMask Green Plasma Membrane) were added to the solutions and incubated for a further 20 min. Then, spheroids were washed twice with PBS and analyzed by confocal microscopy. To reduce the movement of spheroids during the imaging acquisition, they were resuspended in a solution 1:1 v/v of pure FBS and glycerol.

#### 5. Characterization of Spheroids and Data Analysis.

- 5.1. Slices of spheroids were analyzed by means of TEM. The TEM observations of the grids were performed with a ZEISS Libra 120 PLUS operating at 120 kV and equipped with an in-column

Omega filter. Images were analyzed using Fiji-ImageJ software version 1.51s.

- 5.2. Confocal analysis was performed with Olympus FV1000 inverted confocal laser scanning microscope equipped with a thermostat chamber set at 37 °C and 5% CO<sub>2</sub>. The lasers for excitation were 405, 488, and 633 nm. All images were analyzed using Fiji-ImageJ software version 1.51s.

### ■ TIMING

#### Step 1. Preparation of cell suspensions

- Subculturing = 3–4 days until 80–90% of cell confluency
- Cell suspension and counting = 30 min

#### Step 2. Make drops to form cell aggregates

- Drops preparation = 30 min

#### Step 3. Transfer drops and induction of spheroids formation

- Transfer = 10 min
- Incubation = 24 h

#### Step 4. Spheroid recovery and preparation for employment

- Collection of spheroids = 10 min
- Treatments = depending on the employment. For TEM characterization, 3 days for polymerization in resin. For confocal evaluation, 1–2 h.

#### Step 5. Characterization of spheroids and data analysis

- TEM analysis = 2–8 h for images collection and 2–6 h for analysis
- Confocal analysis = 2–8 h for images collection and 2–6 h for analysis

### ■ TROUBLESHOOTING

Step 1. Cells in suspensions may settle and form agglomerates that cause the formation of nonhomogeneous spheroids. The whole solution can be aliquoted into several 1.5 mL tubes and occasionally mixed.

Step 2. Flipping the lid can cause the movement and spread of the drops. Be careful in turning the lid; the movement should be done firmly but not too fast or too slow. This is also why it is suggested that the drops are between 10 and 20  $\mu\text{L}$ . Also, the transfer from the hood to the incubator can cause drops to mix if plates are not

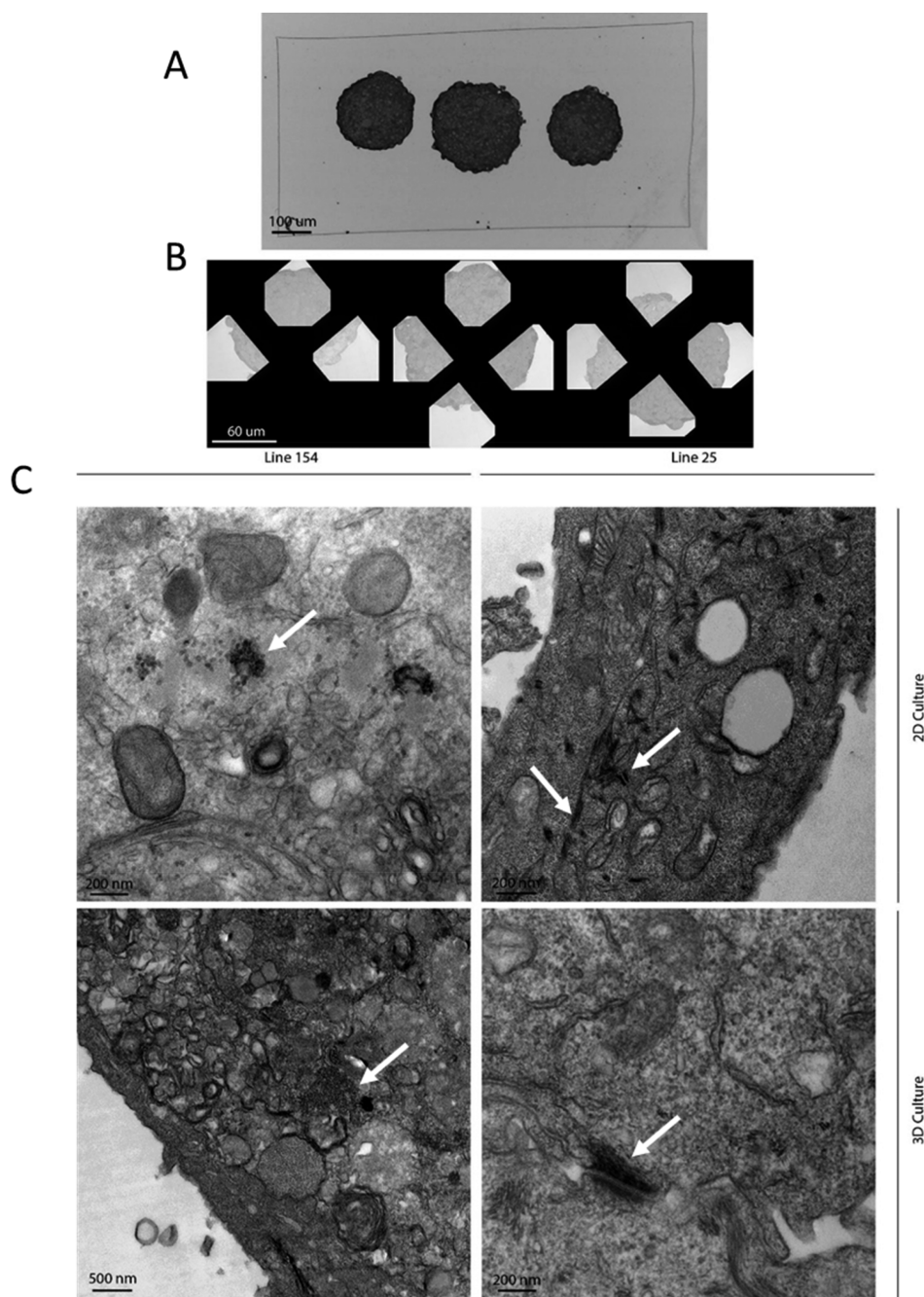


**Figure 5.** Ultrastructural analysis of SCC-25 and UPCI:SCC-154. (A) Sections of SCC-25 spheroids embedded in the resin and visualized with an optical microscope. (B) Sections of SCC-25 spheroids on copper grids visualized by a transmission electron microscope at low magnification mode. (C) Ultrastructural analysis of 2D and 3D culture of SCC-25 and UPCI:SCC-154. Arrows indicate pools of the virus inside UPCI:SCC-154 cells (left column) and tight junctions in SCC-25 (right column).

carefully managed. Sheet formation is strictly dependent on cells; if the sheets are not well-formed after 3 days, try to incubate them for another maximum 24 h and then transfer spheroids or discard them.

Step 3. Sometimes, spheroids may aggregate in the shaker. Maintain a rotating speed  $\geq 70$  rpm to avoid this problem.

Step 4. Each cell line possesses different features, and the spheroids obtained from them can show different cell density and consequently different handling. For each cell line, it is necessary to find the best conditions for the production and handling of the spheroids. If the

spheroids move too much during the acquisition under the confocal microscope, special gels can be used. For example, CyGEL (CY10500, Biostatus) is a novel thermoreversible gel that is compatible with live cells and organisms. It can be used to immobilize spheroids by simple warming at  $37^{\circ}\text{C}$  directly under the microscope if supplied with a thermostated chamber.

## ■ ANTICIPATED RESULTS

The composition of tumor spheroids is fundamental for both the screening of new therapeutics and the basic research on molecular mechanisms that guide tumor growth. On this regard,

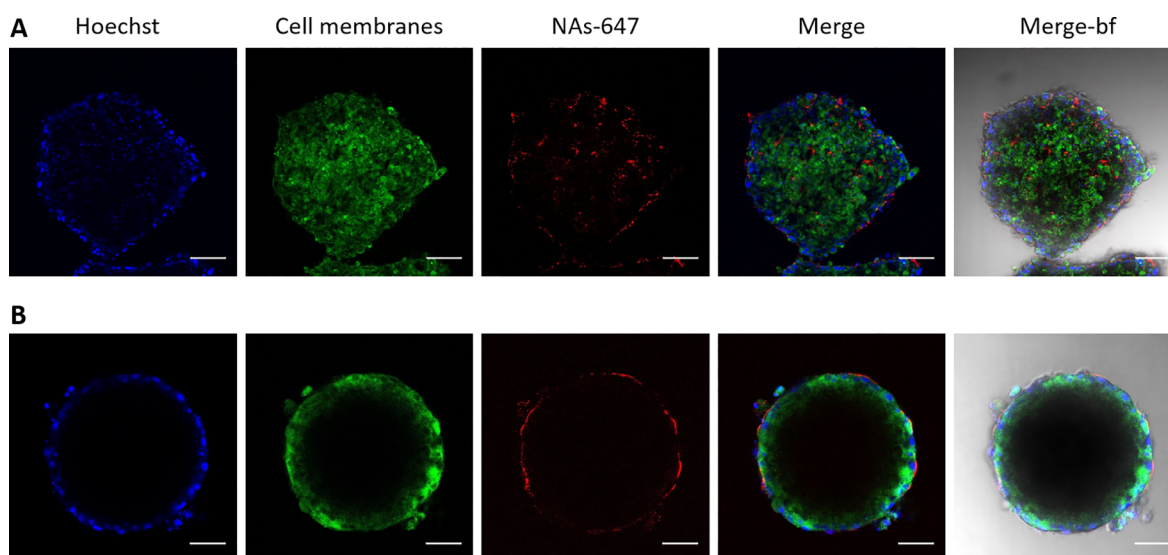


**Figure 6.** Nanoparticles internalization in cells. Dye-labeled nanoarchitectures (NAs-647; containing 3  $\mu\text{g}$  of gold) were used to treat (A) SCC-25 and (B) UPCI:SCC-154 cell lines, and internalization was evaluated by confocal microscopy. From the left to the right column: Nuclei (blue), cell membranes (green), NAs-647 (red), superimposition of nuclei, membranes and nanoparticles, and finally superimposition of all channels with bright field. Scale bar: 100  $\mu\text{m}$ .

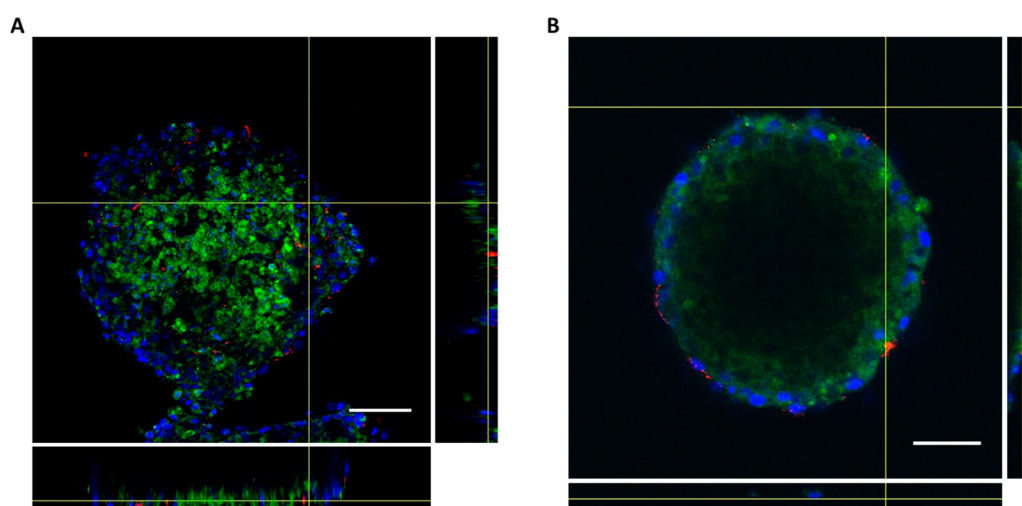


**Figure 7.** Orthogonal view of nanoparticles inside spheroids. Z-stack analysis was performed for (A) SCC-25 and (B) UPCI:SCC-154 spheroids to analyze nanoparticles penetration inside 3D structures. Blue, nuclei; green, cell membranes; red, NAs. Scale bar: 100  $\mu\text{m}$ .

the reproducibility of their production is a key criterion that has been evaluated by assessing the size of different batches of spheroids produced at different times. We obtained an average diameter of  $240.8 \pm 13.3$  and  $199.6 \pm 10.8$   $\mu\text{m}$  for SCC-25 and UPCI:SCC-154, respectively. As also shown in Figures 3 and 4, spheroids obtained from both cell lines have a uniform and spherical shape due to the orbital shaking. Ultrastructural analysis of three-dimensional spheroids leads to the identification of morphological details that could be maintained or lost with respect to the monolayer cell cultures.<sup>27</sup> In the following, the standard protocol for inclusion of spheroids in an appropriate resin is reported together with the TEM analysis (Figure 5). We showed the entire analysis process starting from the cutting of samples embedded inside the resin (Figure 5A). This first step is crucial to understand the quality of the samples, and it allows one to perform a first screening to identify particular areas of interest that can be further analyzed in detail. Then sample slices were placed on a copper grid for TEM

analysis (Figure 5B). For each cell line, we compared cells in 2D or 3D culture conditions (Figure 5C). In the SCC-25 cell line, we found a high number of tight junctions between cells that are also present in the corresponding three-dimensional structures (arrows in the right column). In UPCI:SCC-154 cells, we were able to identify the presence of the virus in the cytosol (arrows in the left column).

In recent years, nanoparticles gained increasing attention as suitable tools for the diagnosis and treatment of neoplasms.<sup>28</sup> Indeed, they have demonstrated some advantages in theranostics, among which increased drug encapsulation features and specific site delivery if properly conjugated with targeting agents.<sup>14</sup> However, it is difficult to understand if nanomaterials are able to be effectively internalized in depth in a tumor by only using 2D cell cultures. In this regard, 3D spheroids resemble neoplasms and their extracellular environment and allow a more effective investigation on the behaviors of nanotherapeutics and their activity. Here, we showed the treatment of spheroids with

dye-labeled gold nanoarchitectures developed by us using an ultrasmall-in-nano approach. Briefly, our nanoparticles are composed of ultrasmall gold seeds (around 3 nm in diameter) embedded in a polymer matrix that is surrounded by a silica shell.<sup>29</sup> These (bio)degradable/excretable nanoarchitectures (NAs) have been employed for the delivery of drugs, development of combined therapies, and imaging purposes.<sup>30–33</sup> As each cell line has different behaviors, we tested whether NAs were able to be internalized in the two HNSCC cell lines composed in the 3D structures. Spheroids were incubated with NAs previously labeled with the fluorophore Alexa Fluor 647 (NAs-647), and their internalization was assessed by confocal microscopy (Figure 6).

Confocal microscopy analyses mainly provide qualitative information about nanoparticle internalization (Figure 6). However, by performing z-stack acquisitions, information on the degree of penetration of nanoparticles inside the spheroids can be successfully achieved (Figure 7). Remarkably, this approach is pivotal to understand the diffusion of NAs inside the 3D structures and to anticipate the potential efficacy of the therapeutic action.

## SUMMARY

Neoplasms represent one of the main causes of death in the world, and among them, HNSCCs are one of the most aggressive.<sup>34</sup> In this regard, SCC-25 and UPCI:SCC-154 are two HNSCC representative cell lines with negative and positive HPV status, respectively. The pharmacological management of HNSCCs, especially for SCC-25, is still mainly based on cisplatin, which causes severe side effects in patients, among which are nephropathologies and increased risk of heart attacks.<sup>35</sup> Indeed, alternative, noninvasive and more effective approaches for treating this class of neoplasms are urgently required. It should also be noted that the neoplasms' complexity is further increased by their unique gene expression, which is peculiar for each cancer and differs from patient to patient as influenced by the lifestyles and the surrounding environment.<sup>36</sup> In this regard, monolayer cell cultures do not sufficiently provide an effective tool for treatment screening. Three-dimensional models, instead, better simulate the behaviors and the boundary conditions of neoplasms, providing reliable platforms for translational research.<sup>37</sup> It is also worth noticing that the integration of 3D neoplasm models into the preclinical research workflow will reduce the use of animal models, in agreement with the 3R's concept. The hanging drop method is one of the most appealing techniques to employ for spheroid production. With respect to other approaches, it allows the production of a high number of spheroids with similar features and without the requirement of any special reagent or equipment, making it particularly suitable for applications such as high-throughput efficacy experiments. Indeed, a single operator can easily produce from 50 to 150 spheroids/day with a success rate of about 70–80%. With the advancement of technological innovation, this technique may be translated to automated systems that allow a further reduction of the costs together with an increased uniformity between spheroids.<sup>38,39</sup> Here, we have described a standard step-by-step protocol for the production of two HNSCC spheroids by employing the hanging drop method. Particular precautions on this models arise from the different SCC-25 and UPCI:SCC-154 growth rates. The resulting 3D models are stable and do not grow (as opposed to other cell lines) after the collection for experiments, probably due to the presence of the surrounding thick layer of the extracellular

matrix (Figures 4 and 5).<sup>14</sup> In this regard, it is worth remembering that this protocol has been optimized for SCC-25 and UPCI:SCC-154 because of the strong demand of advancements for the management of head and neck neoplasms. The translation of our protocol to other cell lines may require further improvements. Interestingly, the presence of the virus inside UPCI:SCC-154 has been confirmed by ultrastructure analysis (Figure 5C). The application of 3D models for the qualitative assessment of nanomaterial internalization has been reported (Figure 6). The optical evaluation of nanoarchitecture distribution is of pivotal importance as the complex structures of spheroids, comprising the presence of the extracellular matrix and the cell–cell interactions, can affect the cellular uptake.

In conclusion, we have comprehensively described a protocol for the high-throughput production of 3D spheroids of two representative HNSCC cell lines, SCC-25 and UPCI:SCC-154, in order to provide a platform to enhance advances on their management. We have also presented two standard assays for the characterization and preliminary employment. These models represent an excellent starting point for new treatment evaluation in oncology.

## AUTHOR INFORMATION

### Corresponding Authors

**Melissa Santi** – Center for Nanotechnology Innovation@NEST, Istituto Italiano di Tecnologia, 12-56126 Pisa, Italy;  
orcid.org/0000-0002-9374-883X; Email: melissa.santi@nano.cnr.it

**Valerio Voliani** – Center for Nanotechnology Innovation@NEST, Istituto Italiano di Tecnologia, 12-56126 Pisa, Italy;  
orcid.org/0000-0003-1311-3349; Email: valerio.voliani@iit.it

### Authors

**Ana Katrina Mapanao** – Center for Nanotechnology Innovation@NEST, Istituto Italiano di Tecnologia, 12-56126 Pisa, Italy; NEST-Scuola Normale Superiore, 12-56126 Pisa, Italy

**Valentina Cappello** – Center for Nanotechnology Innovation@NEST, Istituto Italiano di Tecnologia, 12-56126 Pisa, Italy

Complete contact information is available at:

<https://pubs.acs.org/10.1021/acsbmaterials.0c00617>

### Notes

The authors declare no competing financial interest.

## ACKNOWLEDGMENTS

The research leading to these results has received funding from AIRC under MFAG 2017 – ID 19852 project – P.I. Voliani Valerio. Figures 1 and 2 and the Table of Content Entry have been created with BioRender.com.

## REFERENCES

- (1) Siegel, R. L.; Miller, K. D.; Jemal, A. Cancer Statistics, 2019. *Ca-Cancer J. Clin.* **2019**, *69* (1), 7–34.
- (2) Bose, P.; Brockton, N. T.; Dort, J. C. Head and Neck Cancer: From Anatomy to Biology. *Int. J. Cancer* **2013**, *133* (9), 2013–2023.
- (3) Jung, Y.-S.; Najy, A. J.; Huang, W.; Sethi, S.; Snyder, M.; Sakr, W.; Dyson, G.; Hüttemann, M.; Lee, I.; Ali-Fehmi, R.; Franceschi, S.; Struijk, L.; Kim, H. E.; Kato, I.; Kim, H.-R. C. HPV-Associated Differential Regulation of Tumor Metabolism in Oropharyngeal Head and Neck Cancer. *Oncotarget* **2017**, *8* (31), 51530–51541.

- (4) Busch, C.-J.; Becker, B.; Kriegs, M.; Gatzemeier, F.; Krüger, K.; Möckelmann, N.; Fritz, G.; Petersen, C.; Knecht, R.; Rothkamm, K.; Rieckmann, T. Similar Cisplatin Sensitivity of HPV-Positive and -Negative HNSCC Cell Lines. *Oncotarget* **2016**, *7* (24), 35832–35842.
- (5) Hackenberg, S.; Scherzed, A.; Harnisch, W.; Froelich, K.; Ginzkey, C.; Koehler, C.; Hagen, R.; Kleinsasser, N. Antitumor Activity of Photo-Stimulated Zinc Oxide Nanoparticles Combined with Paclitaxel or Cisplatin in HNSCC Cell Lines. *J. Photochem. Photobiol., B* **2012**, *114*, 87–93.
- (6) Kapalczyńska, M.; Kolenda, T.; Przybyła, W.; Zajączkowska, M.; Teresiak, A.; Filas, V.; Ibbs, M.; Bliźniak, R.; Łuczewski, Ł.; Lamperska, K. 2D and 3D Cell Cultures – a Comparison of Different Types of Cancer Cell Cultures. *Arch. Med. Sci.* **2016**, *14* (4), 910–919.
- (7) Mapanao, A. K.; Voliani, V. Three-Dimensional Tumor Models: Promoting Breakthroughs in Nanotheranostics Translational Research. *Appl. Mater. Today* **2020**, *19*, 100552.
- (8) Duval, K.; Grover, H.; Han, L. H.; Mou, Y.; Pegoraro, A. F.; Fredberg, J.; Chen, Z. Modeling Physiological Events in 2D vs. 3D Cell Culture. *Physiology* **2017**, *32* (4), 266–277.
- (9) Breslin, S.; O'Driscoll, L. The Relevance of Using 3D Cell Cultures, in Addition to 2D Monolayer Cultures, When Evaluating Breast Cancer Drug Sensitivity and Resistance. *Oncotarget* **2016**, *7* (29), 45745–45756.
- (10) Santini, M. T.; Rainaldi, G. Three-Dimensional Spheroid Model in Tumor Biology. *Pathobiology* **1999**, *67* (3), 148–157.
- (11) Lu, H.; Stenzel, M. H. Multicellular Tumor Spheroids (MCTS) as a 3D In Vitro Evaluation Tool of Nanoparticles. *Small* **2018**, *14* (13), 1702858.
- (12) Cassano, D.; Santi, M.; D'Autilia, F.; Mapanao, A. K.; Luin, S.; Voliani, V. Photothermal Effect by NIR-Responsive Excretable Ultrasmall-in-Nano Architectures. *Mater. Horiz.* **2019**, *6* (3), 531–537.
- (13) Nath, S.; Devi, G. R. Three-Dimensional Culture Systems in Cancer Research: Focus on Tumor Spheroid Model. *Pharmacol. Ther.* **2016**, *163*, 94–108.
- (14) Mapanao, A. K.; Santi, M.; Faraci, P.; Cappello, V.; Cassano, D.; Voliani, V. Endogenously Triggerable Ultrasmall-in-Nano Architectures: Targeting Assessment on 3D Pancreatic Carcinoma Spheroids. *ACS Omega* **2018**, *3* (9), 11796–11801.
- (15) Morrissey, B.; Blyth, K.; Carter, P.; Chelala, C.; Jones, L.; Holen, I.; Speirs, V. The Sharing Experimental Animal Resources, Coordinating Holdings (SEARCH) Framework: Encouraging Reduction, Replacement, and Refinement in Animal Research. *PLoS Biol.* **2017**, *15* (1), e2000719.
- (16) Fang, Y.; Eglen, R. M. Three-Dimensional Cell Cultures in Drug Discovery and Development. *SLAS Discovery* **2017**, *22* (5), 456–472.
- (17) Kelm, J. M.; Timmins, N. E.; Brown, C. J.; Fussenegger, M.; Nielsen, L. K. Method for Generation of Homogeneous Multicellular Tumor Spheroids Applicable to a Wide Variety of Cell Types. *Biotechnol. Bioeng.* **2003**, *83*, 173–180.
- (18) Foty, R. A Simple Hanging Drop Cell Culture Protocol for Generation of 3D Spheroids. *J. Visualized Exp.* **2011**, *20* (51), 4–7.
- (19) Hagemann, J.; Jacobi, C.; Hahn, M.; Schmid, V.; Welz, C.; Schwenk-Zieger, S.; Stauber, R.; Baumeister, P.; Becker, S. Spheroid-Based 3D Cell Cultures Enable Personalized Therapy Testing and Drug Discovery in Head and Neck Cancer. *Anticancer Res.* **2017**, *37*, 2201–2210.
- (20) Braunholz, D.; Saki, M.; Niehr, F.; Öztürk, M.; Borràs Puértolas, B.; Korschak, R.; Budach, V.; Tinhofer, I. Spheroid Culture of Head and Neck Cancer Cells Reveals an Important Role of EGFR Signalling in Anchorage Independent Survival. *PLoS One* **2016**, *11* (9), No. e0163149.
- (21) Rheinwald, J. G.; Beckett, M. A. Tumorigenic Keratinocyte Lines Requiring Anchorage and Fibroblast Support Cultured from Human Squamous Cell Carcinomas. *Cancer Res.* **1981**, *41* (5), 1657–1663.
- (22) White, J. S.; Weissfeld, J. L.; Ragin, C. C. R.; Rossie, K. M.; Martin, C. L.; Shuster, M.; Ishwad, C. S.; Law, J. C.; Myers, E. N.; Johnson, J. T.; Gollin, S. M. The Influence of Clinical and Demographic Risk Factors on the Establishment of Head and Neck Squamous Cell Carcinoma Cell Lines. *Oral Oncol.* **2007**, *43* (7), 701–712.
- (23) Pezzini, I.; Marino, A.; Del Turco, S.; Nesti, C.; Doccini, S.; Cappello, V.; Gemmi, M.; Parlanti, P.; Santorelli, F. M.; Mattoli, V.; Ciofani, G. Cerium Oxide Nanoparticles: The Regenerative Redox Machine in Bioenergetic Imbalance. *Nanomedicine* **2017**, *12* (4), 403–416.
- (24) Moscardini, A.; Di Pietro, S.; Signore, G.; Parlanti, P.; Santi, M.; Gemmi, M.; Cappello, V. Uranium-Free X Solution: A New Generation Contrast Agent for Biological Samples Ultrastructure. *Sci. Rep.* **2020**, *10*, 11540.
- (25) Cassano, D.; David, J.; Luin, S.; Voliani, V. Passion Fruit-like Nano-Architectures: A General Synthesis Route. *Sci. Rep.* **2017**, *7*, 43795.
- (26) Cassano, D.; Rota Martir, D.; Signore, G.; Piazza, V.; Voliani, V. Biodegradable Hollow Silica Nanospheres Containing Gold Nanoparticle Arrays. *Chem. Commun.* **2015**, *51* (49), 9939–9941.
- (27) Hess, M. W.; Pfaller, K.; Ebner, H. L.; Beer, B.; Hekl, D.; Seppi, T. *3D versus 2D Cell Culture. Implications for Electron Microscopy*; Academic Press, 2010; Vol. 96.
- (28) Vlamidis, Y.; Voliani, V. Bringing Again Noble Metal Nanoparticles to the Forefront of Cancer Therapy. *Front. Bioeng. Biotechnol.* **2018**, *6*, 143.
- (29) Armanetti, P.; Poció-Martínez, S.; Flori, A.; Avigo, C.; Cassano, D.; Menichetti, L.; Voliani, V. Dual Photoacoustic/Ultrasound Multi-Parametric Imaging from Passion Fruit-like Nano-Architectures. *Nanomedicine* **2018**, *14* (6), 1787–1795.
- (30) Cassano, D.; Summa, M.; Poció-Martínez, S.; Mapanao, A.-K.; Catelani, T.; Bertorelli, R.; Voliani, V. Biodegradable Ultrasmall-in-Nano Gold Architectures: Mid-Period In Vivo Distribution and Excretion Assessment. *Part. Part. Syst. Character.* **2019**, *36* (2), 1800464.
- (31) Avigo, C.; Cassano, D.; Kusmic, C.; Voliani, V.; Menichetti, L. Enhanced Photoacoustic Signal of Passion Fruit-Like Nanoarchitectures in a Biological Environment. *J. Phys. Chem. C* **2017**, *121* (12), 6955–6961.
- (32) Cassano, D.; Santi, M.; Cappello, V.; Luin, S.; Signore, G.; Voliani, V. Biodegradable Passion Fruit-Like Nano-Architectures as Carriers for Cisplatin Prodrug. *Part. Part. Syst. Character.* **2016**, *33* (11), 818–824.
- (33) Cassano, D.; Mapanao, A.-K.; Summa, M.; Vlamidis, Y.; Giannone, G.; Santi, M.; Guzzolino, E.; Pitto, L.; Polisenio, L.; Bertorelli, R.; Voliani, V. Biosafety and Biokinetics of Noble Metals: The Impact of Their Chemical Nature. *ACS Appl. Bio Mater.* **2019**, *2* (10), 4464–4470.
- (34) McDermott, J. D.; Bowles, D. W. Epidemiology of Head and Neck Squamous Cell Carcinomas: Impact on Staging and Prevention Strategies. *Curr. Treat. Options Oncol.* **2019**, *20* (5), 43.
- (35) Lala, M.; Chirovsky, D.; Cheng, J. D.; Mayawala, K. Clinical Outcomes with Therapies for Previously Treated Recurrent/Metastatic Head-and-Neck Squamous Cell Carcinoma (R/M HNSCC): A Systematic Literature Review. *Oral Oncology*; Elsevier Ltd., 2018; pp 108–120.
- (36) Mroz, E. A.; Rocco, J. W. Intra-Tumor Heterogeneity in Head and Neck Cancer and Its Clinical Implications. *World J. Otorhinolaryngol. Neck Surg.* **2016**, *2* (2), 60–67.
- (37) Méry, B.; Rancoule, C.; Guy, J. B.; Espenel, S.; Wozny, A. S.; Battiston-Montagne, P.; Ardail, D.; Beuve, M.; Alphonse, G.; Rodriguez-Lafresse, C.; Magné, N. Preclinical Models in HNSCC: A Comprehensive Review. *Oral Oncology*; Elsevier Ltd. 2017; pp 51–56.
- (38) Raghavan, S.; Ward, M. R.; Rowley, K. R.; Wold, R. M.; Takayama, S.; Buckanovich, R. J.; Mehta, G. Formation of Stable Small Cell Number Three-Dimensional Ovarian Cancer Spheroids Using Hanging Drop Arrays for Preclinical Drug Sensitivity Assays. *Gynecol. Oncol.* **2015**, *138* (1), 181–189.
- (39) Tung, Y. C.; Hsiao, A. Y.; Allen, S. G.; Torisawa, Y. S.; Ho, M.; Takayama, S. High-Throughput 3D Spheroid Culture and Drug Testing Using a 384 Hanging Drop Array. *Analyst* **2011**, *136* (3), 473–478.